THE NEW STARE & CHASE PROCEDURE AT THE SWISS OPTICAL GROUND STATION AND GEODYNAMICS OBSERVATORY ZIMMERWALD

J. Rodriguez, E. Cordelli, and T. Schildknecht

Astronomical Institute University of Bern (AIUB), Sidlerstrasse 5, 3012 Bern , Switzerland, Corresponding author email: julian.rodriguez@aiub.unibe.ch

ABSTRACT

The need of precise orbits of resident space objects to prevent collisions suggests the use of laser-ranging measurements for orbit determination and improvement. A major technical challenge is due to the rather small field of view of the laser if compared against other optical systems. Therefore, the lack of precise ephemerides poses a problem for the direct use of the Satellite Laser Ranging system (SLR). The Stare & Chase method attempts to bridge this gap by correcting the pointing of the telescope using a night-tracking camera. The aim of the current work is to determine the minimum requirements, in terms of number and type of observations needed to chase the object with the laser. In particular, the analysis is divided in two main steps. The first is to find the minimum number of measurements needed to generate ephemerides, after an orbit determination procedure, that will allow the tracking of the object within the same pass. The second step of the analysis is developed in order to find the portion of passage to be observed to ensure the re-acquisition of the object during a subsequent pass over the station. So that one can perform, once more, the Stare & Chase procedure to further improve the knowledge of the orbit of the object. All analysis are performed using real data acquired by the SLR system and the night-tracking camera of the Swiss Optical Ground Station and Geodynamics Observatory Zimmerwald (SwissOGS).

Keywords: Stare & Chase, Satellite Laser Ranging (SLR).

1. INTRODUCTION

Current observing systems within the framework of Space Situational Awareness (SSA) include the use of radars, passive-optical telescopes and active-optical, i.e. lasers, for tracking, cataloging and characterization of space debris. If compared against radar or passive-optical, lasers have the advantage that are fast for tracking, accurate and the ranges reach larger distances. On the other hand, there are important limitations such as dependency on weather conditions, energy of emitted pulses (particularly important for non-cooperative targets) and of utmost importance: small field of view (FoV). The last one will unable the tracking of objects with poor ephemerides. In order to overcome such limitation, the coupling of a night tracking camera into the existing ZIMLAT telescope was done [1]. The night tracking camera is intended to correct in real-time the pointing of the laser in pursuance of ranging the object of interest. To exploit the advantages given by the new implemented hardware, a study is conducted revising number, distribution of observations along the observed arc and type of measurement needed for: first, observing the object until it sets within the same pass. Second, the reacquisition of the object for the next passage. Real measurements from the Swiss Optical Ground Station and Geodynamics Observatory Zimmerwald (Swiss OGS) are used along the current work. For validation purposes public predictions in form of Consolidated Prediction Format (CPF), issued by the International Laser Ranging Service (ILRS), are used.

2. METHODOLOGY

The Stare & Chase method using a night tracking camera consists of two modes of observation:

- Staring mode: The system (camera plus telescope) remains fixed in an initial pointing direction waiting for the object to cross the field of view. First observations are gathered and an initial orbit determination is computed.
- Chasing mode: The system follows the object using the latest generated ephemerides coming from an orbit improvement.

For clarity, figure 1 summarizes the procedure performed in the computation of the study cases.

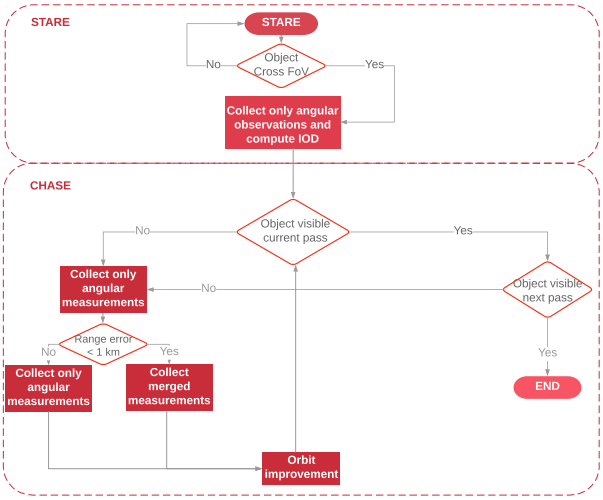

Figure 1. Flowchart Stare & Chase procedure.

The measurements previously collected by ZIMLAT, both those from the SLR system and the tracking camera, are then analyzed in post processing to simulate a stare and chase scenario (figure 1). While in staring mode the system waits until the object crosses the field of view of the tracking camera. Thereafter, a first set of angular observations are collected and used to compute an initial orbit. From the results of the initial orbit determination (IOD), the first set of ephemerides used in the chase mode are generated. During the chasing mode, the system tracks the target using the last generated ephemerides and collects new measurements which will be used to improve the orbit knowledge and therefore update the ephemerides. The assessment of the acquisition of the object, within the same and the next passage, is performed comparing each and every newly generated set of ephemerides against that provided by the ILRS in the CPF. Both sets of ephemerides (AIUB VS CPF) are transformed into topocentric angles (Azimuth and Elevation) and distances. We define total angular error as the angular distance in the sky of the two set of ephemerides, while the range error is defined as the difference between the topocentric distances. The thresholds which discriminate whether or not the object can be tracked, with the night-tracking camera and with the SLR system, are given by the field of view of the camera (FoV, 7 arcmin) and the maximum error, in time of flight, tolerated by the SLR system to distinguish if a received photon belongs to the emitted pulse or if it is just noise. The maximum time of flight error tolerated by our SLR system corresponds to 1 km error in the satellite topocentric distance.
To check whether the satellite can be tracked until the end of the passage, and re-observed for subsequent ones, further conditions are imposed: the elevation of the object must be greater than 15 degrees (elevation mask)[1] and, since we are using a tracking camera that needs of the sunlight reflected by the object, it becomes imperative that the passage must occur during night time [2].The following subsections include a more detailed explanation regarding the algorithms and implementation of the method.

[1] depicted in the plots – section Results – as Visibility window.
[2] depicted in the plots – section Results – as Night time.

2.1. Instruments and Measurements

All observations were provided by the Swiss Optical Ground Station and Geodynamics Observatory Zimmerwald, located 10 km South of Bern, Switzerland. One of the several optical telescopes of the station was used for the current study: Zimmerwald Laser and Astrometry Telescope (ZIMLAT). ZIMLAT (installed in 1997) is used either for laser ranging to satellites or for optical observation of positions and magnitudes of near-Earth objects. During daytime the system operates in SLR mode only. During nighttime the available observation time is shared between SLR and charge-coupled devices (CCD) using negotiated priorities. In addition, light curves and photometric observations can be retrieved. Currently, the night-tracking camera is co-mounted with ZIMLAT; its FoV is 7 arcminutes (further technical description of the hardware can be found in [1]).
To carry out the presented analysis, we used only real measurements collected by the SLR system and the tracking camera of ZIMLAT (for further information please refer to [1]). In order to avoid biases in the interpretation of the results due to the lack of measurements , the analysis was performed on geodetic satellites (LAGEOS-2 and Ajisai) standard targets for an SLR station. Furthermore, in order to find a more general conclusion, three different passes at different elevation over the station (low, medium and high culmination, LC, MC and HC, respectively) were considered for each satellite case. During normal SLR operations the tracking camera was used to adjust the telescope pointing and collect the angular measurements. As reported in [1], the tracking camera provides angular measurements of Azimuth and Elevation without performing an astrometric data reduction. These measurements are, in fact, read directly from the angular encoder of the telescope. The standard deviation of the angular measurements is 6 arcsec [1]. The precision of the SLR system is $\sim$ 1.2 cm –according to the last data quality assessment done by the ILRS [4], however, we consider 50 cm for the ranges to simulate the tracking of an unknown object [3]. These standard deviations are then used in the orbit determination tool as a priori weight of the measurements [3].

2.2. Software

All computations were done using the in-house software CelMech. CelMech is a tool developed for Celestial Mechanics computations of natural and artificial celestial bodies and its Copyright belongs to the Astronomical Institute of the University of Bern. Further information about the tool can be found in [2].

Initial Orbit Determination

The first orbit is computed using the circular orbit assumption. The minimum number of observations for computing a circular orbit is 4 since the solve-for parameters are: the Semi-major Axis, the Inclination, the Right Ascension of the Ascending Node and the Perigee Passing Time.
Within CelMech the program that computes the initial orbit determination is ORBDET. Theoretical aspects about the method plus further details about its implementation can be found in [2].

Orbit Improvement

Each time that an orbit improvement is performed the prior information of the orbit was previously generated using either ORBDET (for first solutions) or SATORB (from previous orbit improvement). Thus, the solve-for parameters for the orbit improvement are corrections to those input orbital elements. The program that computes the orbit improvement and propagates it within CelMech is SATORB.
SATORB performs a batch least-squares adjustment. The latest version of CelMech includes extensions in SATORB that allows the possibility of processing ranges, hence enabling data fusion between different types of observables. Further information is available in [3].

3. RESULTS

In order to find more general results, selected objects, belonging to different orbital regimes and regularly tracked by the ILRS, were chosen for the current study. Those targets are characterized for having good number of observations plus accurate ephemerides in form of CPF. The first satellite is LAGEOS-2 (altitude $\sim$ 5900 km) while the second case is Ajisai (altitude $\sim$ 1488 km).
The observation geometry station-satellite changes with respect to time and differs from one passage to the next one. Three different geometries were chosen matching with passages that correspond to high, medium and low culmination, HC, MC and LC respectively. Each passage will be analyzed independently. Figure 2 and figure 9 show the different passages for the objects of interest. The gaps in the observed passages mean that there is not continue distribution of observations along the arc. Potential reasons for those gaps are: a sudden change in the weather, sensor tasking to observe other visible objects, sun-avoidance maneuver, etc. However, the gaps do not influence the outcome of the current analysis.
For each passage a table summarizes the attempted cases and the compliance of the outcome with the object traceability. The table contains two parts regarding the types and number of observations used for the study case (abbreviated as Meas), plus the results of the computations. The column of measurements is divided into two columns specifying number of angular (abbreviated as Ang) or range measurements (abbreviated as Rg) used for the computation. The column of results is divided showing if the object can be followed until the end of the current pass (labeled as Vis Pass), if the object can be ranged during the current pass (labeled as Rg Pass), if the object is within the FoV for the next passage (labeled as Vis Next), and if the object can be ranged for the next passage (labeled as Rg Next). It is important to note that the first row shows the initial orbit determination (IOD) performed with the number of measurements collected during the staring mode. OI stands for orbit improvement and (*) indicates the number of times that the procedure is repeated. Once the object can be followed until the end of the passage, different observation distribution, using different observables, were selected for maximizing the portion of orbit observed, in order to comply with the aims exposed at the beginning of the current study. The following combination of observations were analyzed:

- Ang Mid uses only angular observations in the middle of the arc.
- Mer Mid uses merged observations in the middle of the arc.
- Ang Mid-End uses only angular observations in the middle and in the end of the arc.
- Ang Mid Mer End uses only angular observations in the middle of the arc and merged in the end.
- Mer Mid-End uses merged observations in the middle and in the end of the arc

It is clear that for using merged observations the condition of the error in range must be satisfied.

3.1. LAGEOS-2

The Laser Geodynamics Satellite - 2 is the second flight unit of the LAGEOS program. Its main mission is the study of the solid Earth through space-geodetic techniques. Its body is a 60 cm diameter sphere with a density of 3.6 g/cm3. The orbital period of LAGEOS-2 is $\sim$ 3.07 hr. The apparent angular velocity is 1.62 arcmin/sec, thus the time that it takes this satellite to cross the FoV of the night tracking camera is $\sim$ 4 seconds. An exposure time of 1 second is selected based on observational experience. For LAGEOS-2, 1 second of exposure time is sufficient to observe the satellite, therefore a maximum of 4 measurements can be collected in the staring mode allowing an IOD. Table 1 and figure 2 show a summary of the passages used for the analysis.

Table 1. Dates and time corresponding to the observed passages.

Passage	Beginning	End
LC	04-OCT-2018 4:06	04-OCT-2018 4:24
MC	05-OCT-2018 2:09	05-OCT-2018 2:49
HC	04-OCT-2018 22:05	04-OCT-2018 22:44

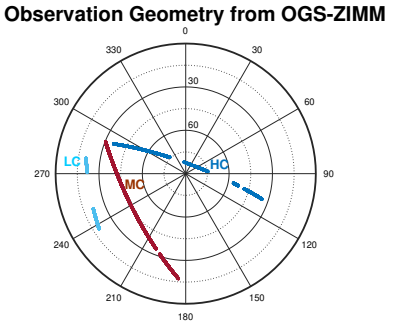

Figure 2. Observation geometry between station-satellite. LC: Low culmination; MC: Medium culmination; HC: High culmination.

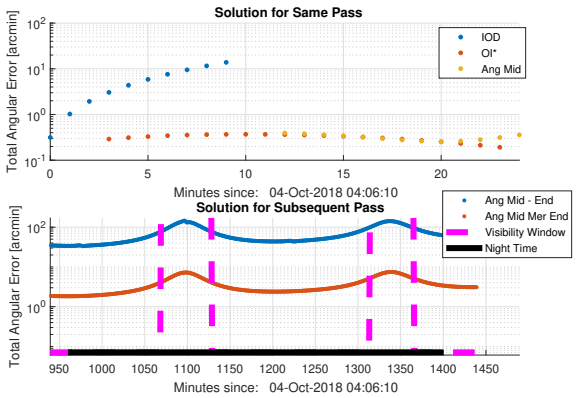

Figure 3. Total angular error LAGEOS-2 for the low culmination case.

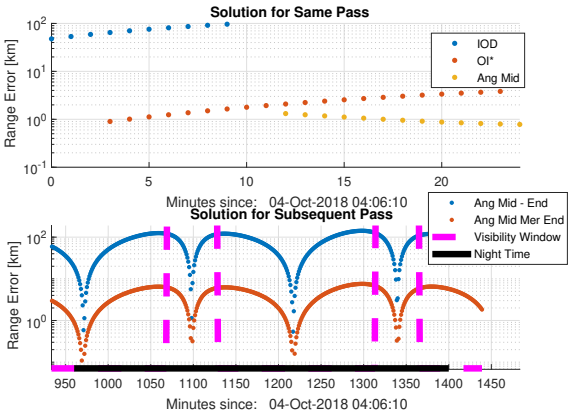

Figure 4. Total angular error LAGEOS-2 for the low culmination case.

Low Culmination

The different results obtained during the analysis of the LC passage are summarized in table 2.
The procedure starts with 4 observations that are the maximum gathered in staring mode with an exposure time of 1 second (IOD). With 4 observations the object can be followed for the next three minutes. *In three minutes 180 observations can be collected and the object can be followed until it sets (OI*).* In this case, 3 minutes are enough to follow the object for the remaining part of the pass, therefore the angular observations are available and can be selected at any time of the observed pass from now on.
In order to be able to range the object, the error in range must not exceed 1 kilometer. As can be seen in the upper plot in figure 4, the solution (OI*) is not sufficient for ranging the object. To overcome such limitation, additional angular observations were added in the middle of the arc (Ang Mid). After the addition of angular measurements in the middle of the arc (minute 12) the object can be ranged at the end of the pass (from minute 21 onwards).
So far, there are available angular observations for the entire pass and ranges at the end of it. For the re-acquisition both solutions are computed – using only angular measurements in the middle and in the end of the arc (Ang Mid-End), and using only angular measurements in the middle and merged in the end (Ang Mid Mer End). The results are shown in the lower plots of figure 3 and 4.

Table 2. Summary of solutions attempted for LAGEOS-2 low culmination passage.

	Meas		Results			
Case	Ang	Rg	Vis Pass	Rg Pass	Vis Next	Rg Next
IOD	4	0	No	No	No	No
OI*	184	0	Yes	No	No	No
Ang Mid	214	0	Yes	Yes	No	No
Ang Mid-End	244	0	Yes	Yes	No	No
Ang Mid Mer End	244	30	Yes	Yes	Yes	No

As it can be seen from figure 3 and 4 the impact of using ranges merged with angular observations is noticeable: a difference in the solution of almost one order of magnitude. In fact, the re-acquisition is achieved by *adding angular observations in the middle of the arc plus merged at the end of it*.

Medium Culmination

The same procedure was repeated for the remaining LAGEOS-2 passages. Table 3 includes the summary of all computed solutions for the medium culmination passage.
The number of observations collected in staring mode does not change for this passage. After this first solution (IOD), 180 observations were collected. In this case, 180 observations are not enough to follow the object until it sets (OI*). Therefore, 30 angular observations are added 1 minute before the object is going to be out of the FoV (OI**). The reason of computing a solution, few minutes before the object will be out of the FoV, is because we considered the processing time of the pipeline. *With 210 observations the object can be tracked within the same*

pass.

The solution OI**, permits the retrieval of ranges until minute 11 (see upper plot figure 6). Once the range error is out of tolerance (minute 16), merged observations, acquired few minutes before, are added (Mer Mid). After adding merged observations in the middle of the arc, the object can be ranged for the remaining part of the pass. Nonetheless, by using only merged measurements in the middle, the object cannot be re-observed for the next pass (lower plot figure 5), thus merged measurements are added in the end of the current passage.

Lowers plots in figure 5 and 6 show that *the solution that uses merged measurements in the middle and end of the arc allows the re-observation of the object*. It must be noticed that the outcome of such combination not only allows the object to be within the FoV of the camera, but allows also to range it in a narrow time-window in the middle of that passage. That is an outstanding result considering the time elapsed between passages, more than 12 hours, the exigent tolerances, the length of the observed arc and the number of observations used for the orbit improvement.

Table 3. Summary of solutions attempted for LAGEOS-2 medium culmination passage.

	Meas		Results			
Case	Ang	Rg	Vis Pass	Rg Pass	Vis Next	Rg Next
IOD	4	0	No	No	No	No
OI*	184	0	No	No	No	No
OI**	214	0	Yes	Yes	No	No
Mer Mid	244	30	Yes	Yes	No	No
Mer Mid-End	274	60	Yes	Yes	Yes	No

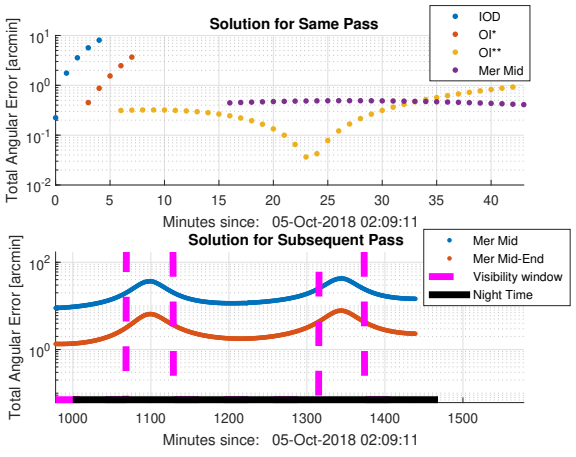

Figure 5. Total angular error LAGEOS-2 for medium culmination case.

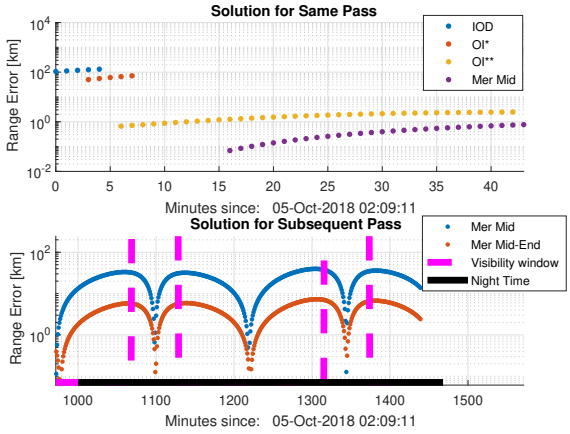

Figure 6. Range error LAGEOS-2 for medium culmination case.

High Culmination

As in the previous cases, the next table shows a summary of the attempted strategies for the high culmination passage of the LAGEOS-2 satellite.

The conclusions from the results of the three previous cases for the medium culmination pass, IOD, OI* and OI**, hold for the current passage. From the upper plot in figure 8, it can be seen that at the beginning of the solution OI** it is possible to range the object for the next 5 minutes. Thereafter, it is possible to perform an orbit improvement either adding only angular or merged observations in the middle of the arc. Those additional measurements, used for the solutions Mer Mid and Mer Mid-End, were added after the first 21 minutes – before the error in range was out of tolerance.

The solution computed using only angular measurements does not meet the specified tolerances, i.e. the object will be out of the field of view, but using merged observations, only in the middle of the arc, yields the re-acquisition of the object for the next pass. It must be noticed that despite the demanding tolerances, in total angular and range error, the re-acquisition is achieved for the next 2 passages. In addition, the object can be ranged during portions of time within those passages.

Table 4. Summary of solutions attempted for LAGEOS-2 high culmination passage.

	Meas		Results			
Case	Ang	Rg	Vis Pass	Rg Pass	Vis Next	Rg Next
IOD	4	0	No	No	No	No
OI*	184	0	No	No	No	No
OI**	214	0	Yes	Yes	No	No
Ang Mid	244	0	Yes	Yes	No	No
Mer Mid	244	30	Yes	Yes	Yes	Yes

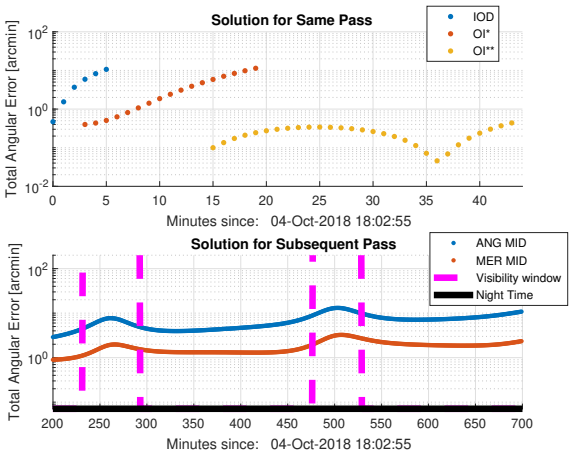

Figure 7. Total angular error LAGEOS-2 for the high culmination case.

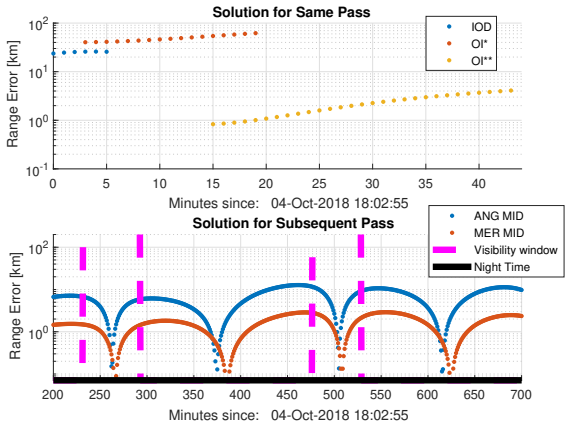

Figure 8. Range error LAGEOS-2 for the high culmination case.

3.2. AJISAI

The Experimental Geodetic Payload (renamed after launch as Ajisai) is a Japanese satellite whose mission has mainly geodetic purposes. Its body is a 2.15 m diameter sphere with a weight of 685 kg. Its orbital period is $\sim$ 1.93 hr. The apparent angular velocity is 3.11 arcmin/sec, thus the time that it takes Ajisai to cross the FoV of the night tracking camera is about 2.25 seconds. The exposure time of 0.1 seconds was set by observational experience. With an exposure time of 0.1 seconds, 22 observations can be collected while the system is in staring mode. The procedure follows the guideline defined in section 2. Table 5 and figure 9 show a summary of the passages used for the analysis.

Table 5. Dates correspondeding to the observed passages.

Passage	Beginning	End
LC	04-SEP-2018 3:57	04-SEP-2018 4:05
MC	08-SEP-2018 00:19	08-SEP-2018 00:31
HC	03-SEP-2018 19:46	03-SEP-2018 19:58

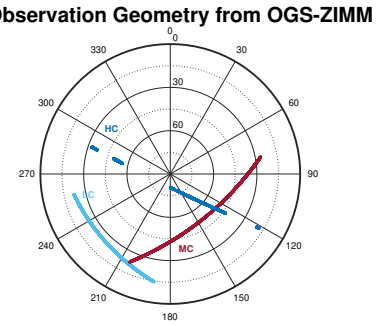

Figure 9. Observation geometry between station-satellite. LC: Low culmination; MC: Medium culmination; HC: High culmination.

Low Culmination

A summary of the analyzed cases for the low culmination passage of Ajisai are shown in table 6. While in staring mode, 22 observations were collected, but the object could only be followed for the next minute (IOD). During this minute observations at a rate of 10 Hz were stored, but only one observation every second is used in an orbit improvement (OI*). *With all angular observations collected during that minute, plus the initial ones collected while in staring mode, it is possible to follow the object for the current pass.*

In order to range the object, angular measurements were added at minute 4 (Ang Mid). As it can be seen in the upper plot in figure 11, the object can be ranged from now on.

At this point, it is possible to use only angular observations in the middle and in the end (Ang Mid-End), or only angular in the middle and merged in the end of the arc (Ang Mid Mer End). From the lower plots in figure 10 and 11 it can be seen that the reacquisition for the next passage is not possible using neither of the previous strategies. However, it should be noticed that the elapsed time between current and next passage is almost 15 hr, and that the next passage correspond to a zenith one; for how we defined the total angular error, it increases with elevation.

If the elapsed time between successive passages would be shorter, e.g. 115 min (approximate orbital period of the satellite), it will be possible to re-observe and range with the specified system. Another alternative may be

the tasking of further stations for which the generated ephemerides are still within their observation tolerances. In such case, the orbit improvement will not only benefit from the re-observation of the passage, but also from the different observation geometry.

Table 6. Summary of solutions attempted for Ajisai low culmination passage.

	Meas		Results			
Case	Ang	Rg	Vis Pass	Rg Pass	Vis Next	Rg Next
IOD	22	0	No	No	No	No
OI*	82	0	Yes	Yes	No	No
Ang Mid	112	0	Yes	Yes	No	No
Ang Mid-End	142	0	Yes	Yes	No	No
Ang Mid Mer End	142	30	Yes	Yes	No	No

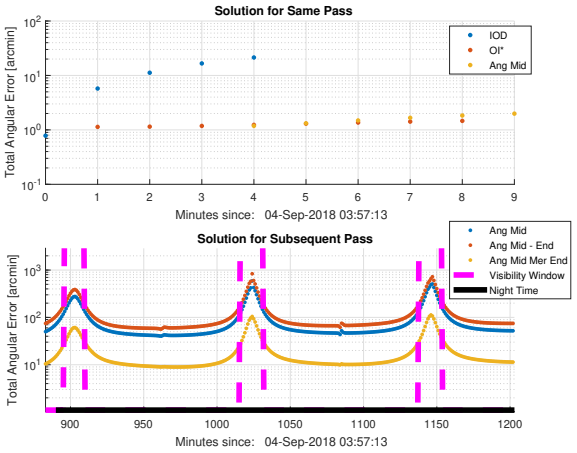

Figure 10. Total angular error AJISAI for the low culmination case.

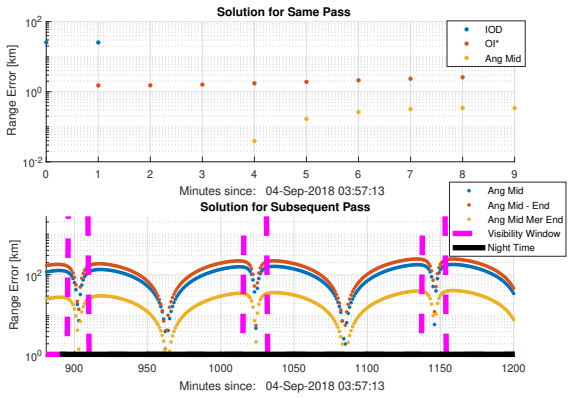

Figure 11. Range error AJISAI for the low culmination case.

Medium Culmination

A summary of the results for the Ajisai medium culmination passage can be seen in table 7. As before, the minimum number of observations collected during staring mode is 22 (IOD). With those 22 angular observations the object could be followed for 4 minutes (see upper plot figure 12). One minute before the object will be out of the field of view, an orbit improvement is performed using all angular observations collected until then. The collected 1800 observations were sampled to 180 since the usage of the entire set of measurements was not improving the accuracy of the solution. *The orbit improvement using the sampled 180 angular measurements, plus those collected during staring mode (22), allows to follow the object until it sets.*

Using the ephemerides generated by the OI* solution, we can range the object from the 4th minute until the end of the passage (see upper plot in figure 13).

To re-observe the object ranges and angular measurements, plus any combination thereof, can be used in an orbit improvement calculation. As expected, the best solution is achieved by the combination of merged measurements in the middle and in the end of the arc. However, even if using the solution Mer Mid-End, the object will be out of the FoV after the 4th minute of the subsequent passage. In that situation it might be advisable to perform the Stare & Chase procedure once more, gathering the observations from the previous passage plus those provided while the object was within the FoV of the next pass.

Table 7. Summary of solutions attempted for Ajisai medium culmination passage.

	Meas		Results			
Case	Ang	Rg	Vis Pass	Rg Pass	Vis Next	Rg Next
IOD	22	0	No	No	No	No
OI*	202	0	Yes	Yes	No	No
Ang Mid	232	0	Yes	Yes	No	No
Mer Mid	232	30	Yes	Yes	No	No
Ang Mid-End	262	0	Yes	Yes	No	No
Ang Mid Mer End	262	30	Yes	Yes	No	No
Mer Mid-End	262	60	Yes	Yes	Yes	No

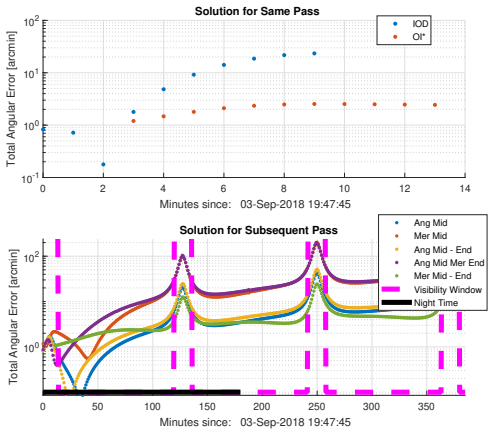

Figure 12. Total angular error AJISAI for the medium culmination case.

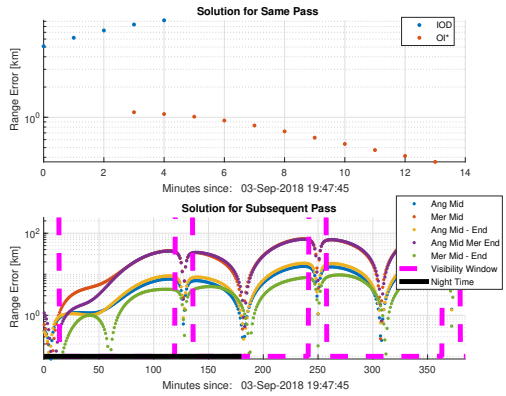

Figure 13. Range error AJISAI for the medium culmination case.

High Culmination

The results of the high culmination passage of Ajisai are shown in table 8. As usual, the 22 angular observations acquired during the staring mode allow to follow the object for the next minute (IOD).
Due to the correlation between measurements, as in the medium culmination case, only 60 measurements out of 600, distributed along the minute when the satellite is still within the FoV, are used for an orbit improvement (OI*). After an orbit improvement with the sampled measurements, the object could be tracked for the next three minutes. During that time it was possible to collect additional 1800 observations. *The orbit improvement using the sampled 262 angular observations (OI**) enables to see the object until the end of the pass (upper plot figure 14).*
The solution, given by the orbit improvement OI**, enables the system to acquire ranges after the second minute (top subplot figure 15). Similarly to the previous passage, all possible combinations (type of observable and distribution of observations along the arc) were computed.
The lower subplots in figure 14 and 15 give an idea of the order of magnitude of the error for the different computed solutions. The best solution (Mer Mid-End), which is one order of magnitude better than the others, is the only one that ensures the re-observation of the object (also with ranges) in the subsequent pass.

Table 8. Summary of solutions attempted for Ajisai high culmination passage.

	Meas		Results			
Case	Ang	Rg	Vis Pass	Rg Pass	Vis Next	Rg Next
IOD	22	0	No	No	No	No
OI*	82	0	No	No	No	No
OI**	262	0	Yes	Yes	No	No
Ang Mid	292	0	Yes	Yes	No	No
Mer Mid	292	30	Yes	Yes	No	No
Ang Mid-End	322	0	Yes	Yes	No	No
Ang Mid Mer End	322	30	Yes	Yes	No	No
Mer Mid-End	322	60	Yes	Yes	Yes	Yes

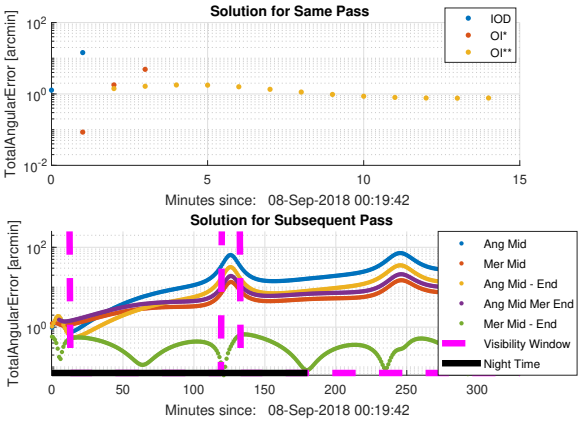

Figure 14. Total angular error AJISAI for the high culmination case.

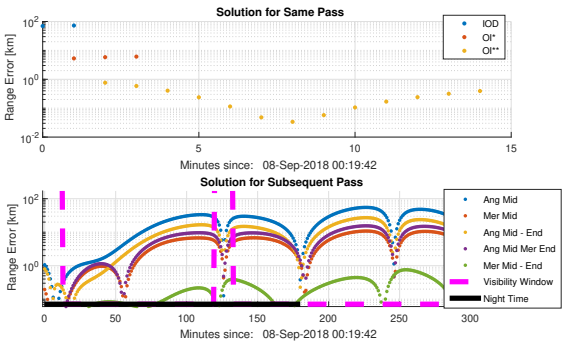

Figure 15. Range error AJISAI for the high culmination case.

4. DISCUSSION & CONCLUSIONS

A new night-tracking camera was installed in the ZIMLAT telescope. The night tracking camera corrects the pointing of the telescope in order to allow the tracking with the SLR system of those objects with poor ephemerides. In the current study we analyzed the number of observations, their distribution along the arc and their type in order to be able to track, with the SLR system, a presumed unknown object within the current and the subsequent passes. For the study only real measurements collected by the SwissOGS SLR system and the ZIMLAT night-tracking camera were used. The study was performed on LEO and MEO ILRS geodetic satellites, Ajisai and LAGEOS-2, respectively.

From the current study, it was proved that the observations gathered in the staring mode (4 and 22 observations for LAGEOS-2 and Ajisai, respectively) were enough to start the observation and ephemerides generation procedure, which allowed the tracking of the object within the same pass.

For LAGEOS-2 (MEO case), less than 3.5 minutes of continuous observations are enough to track the satellite until it sets. Usually, the addition of angular measurements in the middle of the pass allows to range the satellite, using the SLR system, within the same pass. Adding only 30 seconds of measurements, both angular and ranges, in the middle (Mer Mid case HC passage), and in the middle and end of the pass (Mer Mid-End case MC passage) enabled the re-observation of the object for the subsequent passes.

For Ajisai (LEO case), the ephemerides generated from the IOD guarantees at least one minute of further observations. The measurements collected after the first orbit improvement ensures at least the tracking of the object for half of the pass. The subsequent orbit improvement allows, both the tracking and the ranging, of the object within the same pass. The solution that allows the re-observation of the object for the next passage is the one that uses merged observations in the middle and in the end of the pass.

In general, we can say that the measurements acquired in the staring mode are enough to follow (iteratively) the object until it sets. The distribution of only angular measurements within the first half of the pass allows to range the object within the same pass. The re-observation during subsequent passes is guaranteed by the maximization of the observed portion of the pass. As expected, the best solution is given by the processing of observations collected at the beginning, middle, and the end of the arc. The processing of merged measurements (even using few ranges only) improves the accuracy of the estimated orbit by one order of magnitude, in the best case. The synergy between observables must be highlighted and recommended for orbit determination/improvement whenever it is possible.

With a view in the near future, next steps are briefly summarized. Since it was proven that the Stare & Chase procedure can be performed with our system, the next step will be the full automation of the procedure. However, due to the limitation introduced by the FoV of the tracking camera, we will study and implement an orbit improvement capability which exploits the existing a priori knowledge of an object and improve a subset of the solve-for parameters in the orbit determination. Once implemented such strategy, an observation campaign will be performed for validation.

ACKNOWLEDGMENTS

The first author would like to acknowledge the Swiss National Science Foundation for providing the funds for the study. The support from the staff of the Optical Ground Station and Geodynamics Observatory Zimmerwald is highly appreciated.

REFERENCES

1. Cordelli E., Schlatter P., Lauber P., Schildknecht T. Use of a night-tracking camera for real time corrections of the pointing of the SLR system. 21st International Workshop on Laser Ranging, Canberra, Australia, November 2018, http://cddis.gsfc.nasa.gov/lw21/.
2. Beutler G., Mervart L.(2010). *Methods of celestial mechanics*, Springer, 2nd printing.
3. Cordelli E.. Improvements of Space Debris Orbits. PhD thesis, 2017.
4. Internation Laser Ranging Service (ILRS). *SLR Global Performance Report Card.* `https://ilrs.cddis.eosdis.nasa.gov/network/system_performance/global_report_cards/monthly/perf_201809_wLLR.html`. Web. Date of access: 15-JAN-2019.